SPANDIDOS PUBLICATIONS

ONCOLOGY REPORTS 52: 135, 2024

Pituitary tumor-transforming gene 1 regulates the senescence and apoptosis of oral squamous cell carcinoma in a p21-dependent DNA damage response manner

SUYEON PARK[1], SHIHYUN KIM[1], MOON-YOUNG KIM[2], SANG SHIN LEE[1*] and JONGHO CHOI[1*]

[1]Department of Oral Pathology, College of Dentistry, Gangneung-Wonju National University, Gangneung-si, Gangwon-do 25457, Republic of Korea; [2]Department of Oral and Maxillofacial Surgery, College of Dentistry, Dankook University, Dongnam-gu, Cheonan 31116, Republic of Korea

Received March 26, 2024; Accepted June 6, 2024

DOI: 10.3892/or.2024.8794

Abstract. Pituitary tumor-transforming gene 1 (PTTG1), also known as securin, is a proto-oncogene involved in the development of various cancers by promoting cell proliferation and mobility. However, its underlying biological mechanisms in oral squamous cell carcinoma (OSCC) progression remain unclear. in the present study, it was sought to elucidate the role of PTTG1 as an oncogene in OSCC progression and was attempted to unravel the underlying mechanism and impact of PTTG1 expression on cell cycle, cell death, and cellular senescence. The effect of double strand break on PTTG1 expression was investigated in OSCC growth. To identify the role of PTTG1 in OSCC growth, the cell viability and senescence was analyzed by EdU and senescence-associated beta-galactosidase (SA-β-gal) assay, respectively. To verify the DNA damage-induced senescence of PTTG1, the chromosomal damage in OSCC was analyzed *in vitro*. Finally, the effect of PTTG1 on tumor growth and gene expression related to cell viability and DNA damaged-induced senescence was investigated *in vivo*. PTTG1 expression was compared between OSCC and healthy patient samples (n=32) using reverse transcription-quantitative PCR and immunohistochemistry; and it was found that PTTG1 expression was upregulated in OSCC. Small interfering RNA-mediated knockdown of PTTG1 in two OSCC cell lines revealed that PTTG1 downregulation significantly inhibited cell proliferation and arrested the cell cycle pathway as evidenced by changes in checkpoint genes (such as cyclin D1, E and B1). PTTG1 knockdown also increased apoptosis, as evidenced by the upregulation of apoptotic genes [such as cleaved (c-) Caspase-7 and c-poly (ADP-ribose) polymerase]. Moreover, PTTG1 downregulation promoted cellular senescence, as shown by western blotting and SA-β-gal staining. Finally, senescence-induced DNA damage was observed in OSCC cells, which accelerates genomic instability, through chromosomal damage analysis. Taken together, the present findings suggested that PTTG1 acts as a proto-oncogene; regulates cell proliferation, cell cycle, cellular senescence and DNA damage in OSCC; and may serve as a novel diagnostic biomarker and potential therapeutic target for OSCC.

Correspondence to: Professor Jongho Choi, Department of Oral Pathology, College of Dentistry Gangneung-Wonju National University, 7 Jukheon-gil, Gangneung-si, Gangwon-do 25457, Republic of Korea
E-mail: jhchoi@gwnu.ac.kr

[*]Contributed equally

Abbreviations: OSCC, oral squamous cell carcinoma; PTTG1, pituitary tumor-transforming gene 1; SA-β-gal, senescence-associated beta-galactosidase; c-, cleaved-; Cas7, Caspase-7; PARP, poly (ADP-ribose) polymerase; PCNA, proliferating cell nuclear antigen; GAPDH, glyceraldehyde 3-phosphate dehydrogenase; γH2AX, phosphorylated histone H2AX; ATM, ataxia telangiectasia mutant; ATR, ataxia telangiectasia and Rad3-related protein; siRNA, small interfering RNA; IHC, immunohistochemistry; TUNEL, terminal deoxynucleotidyl-transferase-mediated dUTP nick end labeling; RT-qPCR, reverse transcription-quantitative polymerase chain reaction; EdU, 5-Ethynyl-2'-deoxyuridine; RT, room temperature

Key words: OSCC, PTTG1, p21, cellular senescence, DNA damage

Introduction

Oral squamous cell carcinoma (OSCC), the most common type of head and neck cancer, primarily occurs in the oral cavity and lips (1). Data from the Global Cancer Observatory revealed that the worldwide incidence and mortality of OSCC in 2020 were ~380,000 (2.0%) and 180,000 (1.8%), respectively, and are predicted to increase by 47% by 2040 (2). The standard treatment approach for OSCC involves surgical resection followed by adjuvant radiotherapy or chemoradiotherapy depending on the disease stage (3). However, despite advancements in treatment modalities, the 5-year survival rate of OSCC remains stagnant, and the adverse effects of these therapies cannot be ignored (4). For example, because chemotherapy is primarily administered intravenously to non-specific tissues in the body, it may cause collateral damage to healthy

tissues as it causes substantial toxicity to normal cells, leading to severe side effects (5). Moreover, even though irradiation is effective in treating tumor cells by inducing senescence, it poses a potential risk of carcinogenesis by inducing senescence in the surrounding normal cells (6). Therefore, it is necessary to develop alternative OSCC-specific therapies and identify novel biomarkers for the treatment of OSCC. To accomplish this, it is necessary to investigate the underlying mechanisms of the disease.

Pituitary tumor-transforming gene 1 (PTTG1) is a transcription factor ubiquitously expressed, excluding the testes, and mainly participates in regulating sister chromatid separation during cell division and aneuploidy (7,8). PTTG1 overexpression has been reported in various tumor types and is involved in genetic instability, playing an oncogenic role in tumorigenesis (9-11). PTTG1 induces DNA damage in cervical cancer cells through its involvement in genome instability, ultimately promoting cell apoptosis (12). Furthermore, PTTG1 overexpression stimulates *c-Myc* expression by interacting with p53 and is involved in sister chromatid separation or the inhibition of DNA damage repair by inducing chromosomal instability (13-16). Regarding its role in OSCC, Liao *et al* (17) reported that PTTG1 was markedly overexpressed in the tissues of patients with OSCC. Moreover, Zhang *et al* (18) demonstrated that PTTG1 overexpression promotes epithelial-mesenchymal transition (EMT), which results in OSCC cell migration and invasion regulation. However, the precise role of PTTG1 in OSCC remains unclear and requires further investigation.

Cellular senescence plays a vital role as a tumor-suppressive mechanism during the initial stages of tumor development (19). Currently, this process is referred to as replicative senescence because of the diverse intrinsic and extrinsic stresses that lead to permanent cell cycle arrest (20,21). Senescence prevents the proliferation of damaged cells and differs from apoptosis, which eliminates irreparably damaged cells (22). Senescent cells are commonly characterized by the accumulation of intracellular senescence-associated beta-galactosidase (SA-β-gal) along with morphological alterations, such as enlarged cell size and a flattened shape (23,24). Senescent cells are also characterized by activation of the p21/WAF1 and p16/INK4a signaling pathways, the senescence-associated secretory phenotype (SASP), and DNA damage, which are collectively referred to as senescent phenotypes (25). Senescence was initially considered to be associated with limited cell proliferation in normal cell culture (26). A recent study revealed that cell division cycle 25B (Cdc25B), a cell cycle regulator, triggers cell senescence in a p53-dependent manner, leading to the inhibition of DNA synthesis without affecting apoptosis in normal fibroblast cells (27). Jung *et al* (28) demonstrated that the loss of PTEN by mTOR kinase leads to cell cycle inhibition and cellular senescence induction in breast cancer cells through p53 phosphorylation. However, the potential association among senescence, cell cycle arrest and tumor suppression in OSCC remains poorly understood.

Therefore, the present study aimed to elucidate the role of PTTG1 as an oncogene in OSCC progression and to elucidate the underlying mechanism and impact of PTTG1 expression on cell cycle, cell death and cellular senescence. The present study highlights the significance of PTTG1 as a potential diagnostic and post-treatment biomarker for patients with OSCC.

Materials and methods

Human tissues samples. Tumor and adjacent healthy tissue specimens from 32 patients (24 males and 8 females) with OSCC were obtained from Ganenung-Wonju National University Dental Hospital (Gangneung), Keimyung University Dongsan Hospital (Daegu), Pusan National University (Pusan), Inje Paik University (Pusan), and Korea Biobank Network members (Yongin). All tissue samples were obtained with written informed consent of patients aged 50-75 years (mean age: 62) before surgery, and OSCC was histologically diagnosed by pathologists using tissue fragments from the oral region. The tissues were divided into two sections. One section was fixed in 10% formalin overnight at 25˚C for immunohistochemical (IHC) staining. The other section was frozen immediately in liquid nitrogen, stored at -80˚C and was used for real time-PCR and Western blotting. In total, 32 paired individual samples were randomly pooled into four samples, each containing an equal mass of tissues, for analysis. The present study was approved (approval no. GWNUIRB-2020-26-1) by the Committee for Ethical Review of Research of Gangneung-Wonju National University (Gangneung-si, Korea) and conducted from December 2020 to February 2023.

Cell culture and transfection. The p53 mutant human OSCC cell lines HSC-2, SCC-9 and YD-10B were obtained from the Japanese Collection of Research Bioresources Cell Bank, the American Type Culture Collection and the Korean Cell Line Bank, respectively. All OSCC cell lines were cultured in Dulbecco's modified Eagle's medium (DMEM; Invitrogen; Thermo Fisher Scientific, Inc.) supplemented with 10% (w/v) fetal bovine serum (FBS; Gibco; Thermo Fisher Scientific, Inc.) and 1% penicillin/streptomycin (P/S; Gibco; Thermo Fisher Scientific, Inc.). The cell lines were incubated at 37˚C with 5% CO_2.

For the transient knockdown of PTTG1, small interfering (si)RNA (Invitrogen; Thermo Fisher Scientific, Inc) was used to silence PTTG1 expression. A negative vehicle siRNA plasmid was used as a control (Table SI). Lipofectamine 2000 (Invitrogen; Thermo Fisher Scientific, Inc.) was used for transfection following the manufacturer's protocol. Briefly, OSCC cell lines were transfected with 25 nM PTTG1 siRNA in serum-free media until the cells reached 30-40% confluence. After 6 h of incubation at 37˚C in a 5% CO_2 atmosphere, the medium was replaced with a culture medium, and the cells were incubated overnight before harvesting.

Reverse transcription-quantitative polymerase chain reaction (RT-qPCR) analysis. Total RNA was extracted from OSCC cells transfected with the negative control vehicle or with the PTTG1 siRNA using the TRIzol® reagent (Invitrogen; Thermo Fisher Scientific, Inc.). The isolated RNA was used for cDNA synthesis using the Accupower® RocketScript™ Cycle RT PreMix kit (Bioneer, Inc.) according to the manufacturer's protocol. The thermocycling conditions for cDNA amplification were as follows: 50˚C for 60 min, 95˚C for 5 min, and hold at 4˚C. The RT-qPCR was conducted using the CFX96 Touch

Real-Time PCR Detection System (Bio-Rad Laboratories, Inc.) and the following thermocycling conditions: 95˚C for 3 min, followed by 40 cycles of 95˚C for 15 sec, 60˚C for 30 sec, 95˚C for 15 sec, 65˚C for 5 sec, and 95˚C for 30 sec. The RT-qPCR was performed using primers specific for *PTTG1* (forward, 5'-TGACTCAGGCTGGAAGATTTG-3' and reverse, 5'-GGTGGGAGAAGCAAAGGTATAG-3'), *p21* (forward, 5'-AGGTGGACCTGGAGACTCTCAG-3' and reverse, 5'-TCCTCTTGGAGAAGATCAGCCG-3') and *GAPDH* (forward, 5'-CAAAGTTGTCATGGATGACC-3' and reverse, 5'-CCATGGAGAAGGCTGGGG-3'). The $2^{-\Delta\Delta Cq}$ method was used for the relative quantification of gene expression (29). The mRNA levels of the target genes were normalized to that of *GAPDH*. Independent experiments were conducted in triplicates.

Western blotting. For protein isolation, OSCC samples (vehicle control and siRNA) were lysed in Laemmli buffer supplemented with a protease inhibitor cocktail (Roche Diagnostics). The protein concentration was measured using a BCA kit (Thermo Fisher Scientific, Inc.). An equal amount of proteins (50 μg) were separated by sodium dodecyl sulfate-polyacrylamide gel electrophoresis (SDS-PAGE) using an 8-15% acrylamide gel at 100 V for ~2 h and 30 min. The separated proteins were transferred to 0.45-μm nitrocellulose membranes (Bio-Rad Laboratories, Inc.) at 20 V overnight. The membranes were blocked in 5% (w/v) bovine serum albumin (BSA; Sigma-Aldrich; Merck KGaA) dissolved in phosphate-buffered saline (PBS) containing 0.01% Tween-20 (PBS-T) for 1 h at room temperature (RT, 15-25˚C) and then washed with 0.05% PBST. Next, the membranes were incubated with the following primary antibodies overnight at 4˚C: Rabbit anti-PTTG1 (cat. no. GTX111938; GeneTex, Inc.), anti-p21 (cat. no. 2947; Cell Signaling Technology, Inc.), anti-p53 (cat. no. 2527; Cell Signaling Technology, Inc.), anti-retinoblastoma (Rb; cat. no. 9390; Cell Signaling Technology, Inc.), anti-phosphorylated Rb (cat. no. 8180; Cell Signaling Technology, Inc.), anti-proliferating cell nuclear antigen (PCNA; cat. no. 2586; Cell Signaling Technology, Inc.), mouse anti-Caspase-7 (Cas-7; cat no. sc-56063; Santa Cruz Biotechnology, Inc.), anti-cleaved (c-) Cas-7 (cat. no. 8438; Cell Signaling Technology, Inc.), anti-c-poly (ADP-ribose) polymerase (PARP; cat. no. 5625; Cell Signaling Technology, Inc.), anti-PARP (cat. no. 9542; Cell Signaling Technology, Inc.), mouse anti-cyclin D1 (cat. no. sc-450; Santa Cruz Biotechnology, Inc.), mouse anti-cyclin E (cat. no. sc-247; Santa Cruz Biotechnology, Inc.), mouse anti-cyclin B1 (cat. no. sc-245; Santa Cruz Biotechnology, Inc.), anti-phosphorylated histone H2AX (γH2AX; cat. no. 80312; Cell Signaling Technology, Inc.), anti-phosphorylated ATR (cat. no. 2853; Cell Signaling Technology, Inc.) anti-ATR (cat. no. 2790; Cell Signaling Technology, Inc.), anti-phosphorylated ataxia telangiectasia mutant (p-ATM; cat. no. 13050; Cell Signaling Technology, Inc.) and anti-ATM (cat. no. 2873; Cell Signaling Technology, Inc.); all primary antibodies were diluted at 1:1,000 with BSA. GAPDH (cat. no. LF-PA0018; AbFrontier Co., Ltd.; 1:3,000 dilutions in BSA) was used as a loading control. After washing three times with PBST, the membranes were incubated with horseradish peroxidase-conjugated secondary antibodies against rabbit (cat. no. 7074P2; Cell Signaling Technology, Inc.) or mouse IgG (cat. no. 7076P2; Cell Signaling Technology, Inc.) at a dilution of 1:5,000 in BSA for 1 h at RT. Protein bands were visualized using a FUSION Solo S imaging system (Vilber China) with an enhanced chemiluminescence reagent (cat. no. WBLUF0100; Merck KGaA). Protein expression was quantified in triplicate using ImageJ software (version 1.53a; National Institutes of Health), and the intensity of the bands was calculated as fold change. The expression levels of phosphorylated proteins were normalized to the total form of each protein. This experiment was repeated thrice.

IHC. Paraffin-embedded OSCC tissues were sectioned into 4-μm sections and placed onto coated slides and fixed in 4% paraformaldehyde overnight at RT. Next, the sections were dewaxed in xylene for 20 min and dehydrated in a graded ethanol series for 1 min each. After incubating in 3% H_2O_2 for 30 min, the samples were washed with PBS and incubated in sodium sulfate buffer (pH 6.0) at RT for antigen retrieval. The samples were blocked with 5% (w/v) BSA for 30 min at RT and washed three times with PBS. Subsequently, the samples were incubated with rabbit anti-PTTG1 antibody (cat. no. GTX111938; GeneTex, Inc.; 1:500 dilutions in BSA) at 4˚C overnight. Tissues were washed three times with PBS and incubated with biotinylated goat anti-rabbit (1:1,00; cat. no. 7074P2; Cell Signaling Technology, Inc.) or anti-mouse IgG (1:1,000; cat. no. 7076P2; Cell Signaling Technology, Inc.) for 1 h at RT. The samples were washed thrice with PBS and incubated with diaminobenzidine (DAB; Abcam). Subsequently, the samples were counterstained with hematoxylin (Dako; Agilent Technologies, Inc.) and dehydrated using a graded ethanol and xylene series before mounting in Canada balsam mixture (cat. no. 2525-4405; Sigma-Aldrich; Merck KGaA). All observations were performed using an upright microscope (BX53; Olympus Corporation) equipped with an objective lens (x10).

Immunofluorescence. To explore chromosomal damage in OSCC cells, $3x10^4$ cells were cultured in Opti-MEM media (Gibco; Thermo Fisher Scientific, Inc.) on coverslips and transfected with 25 nM vehicle control or siRNA-PTTG1 at a density of 30-40%. The following day, the cells were transferred to culture media, cultured overnight, fixed with 4% paraformaldehyde, permeabilized with 0.5% Triton X-100 (Sigma-Aldrich; Merck KGaA) for 15 min at RT, and then washed twice with PBS for 3 min. After incubation with the primary antibody against γH2AX (1:500; cat. no. 80312; Cell Signaling Technology, Inc.) at 4˚C overnight, the coverslips were washed with PBS and incubated with a secondary goat anti-mouse antibody conjugated with Alexa Fluorescence 488 (1:1,000; cat. no. A32723; Invitrogen; Thermo Fisher Scientific, Inc.). Images were acquired using a confocal microscope (STELLARIS 5; Leica Microsystems, Inc.) equipped with an oil objective lens (x63). Z-stacks were used in three confocal images and merged using the ImageJ software. The experiment was performed in triplicate.

5-Ethynyl-2'-deoxyuridine (EdU) assay. To detect cell proliferation in OSCC, an EdU staining Proliferation kit (cat. no. C10337; Fluor 488, Invitrogen; Thermo Fisher Scientific, Inc.) was used following the manufacturer's protocol. A total of $5x10^4$ cells were plated on 12-mm

coverslips in serum-free media and incubated overnight. The cells were transfected with vehicle control or siRNA-PTTG1 at a density of 30-40% in Opti-MEM media (Gibco; Thermo Fisher Scientific, Inc.) for 6 h and the culture medium was changed. After 24 h, 2 μg/ml EdU was added, and the cells were cultured in 5% CO_2 at 37˚C for 2 h. The cells were fixed, permeabilized with 4% paraformaldehyde and 0.5% Triton X-100 (Sigma-Aldrich; Merck KGaA) for 15 min at RT, stained with 500 μl Click-iT reaction buffer for 1 h at RT, and mounted with a Fluorshield Mounting Medium containing DAPI (cat. no. ab104139; Abcam) for 15 min at RT. For quantification, at least seven images were randomly obtained using a fluorescence microscope (BX53; Olympus Corporation) with a x40 objective lens. The experiments were performed in triplicate.

SA-β-gal staining. To investigate the cellular senescence of the OSCC cells, a SA-β-gal staining kit (cat. no. 9860; Cell Signaling Technology, Inc.) was used following the manufacturer's protocol. The cells were seeded in 6-well plates at $5x10^4$ cells per well, allowed to attach overnight, treated with either vehicle control or siRNA-PTTG1 at 25 μM in Opti-MEM media (Gibco; Thermo Fisher Scientific, Inc.) for 6 h, and cultured overnight. The cells were then fixed in the fixation solution for 15 min, washed twice with PBS, and incubated with SA-β-gal staining solution for 12 h at 37˚C. For quantification, at least seven images were randomly acquired using an inverted light microscope (BX53; Olympus Corporation) at x40 magnification. Independent experiments were conducted in triplicate.

Human OSCC xenograft model. A total of $2x10^6$ HSC-2 and SCC-9 cells treated with vehicle control or siRNA-PTTG1 were randomly divided and injected into independent groups of 5 BALB/c-nu/nu male nude mice (total n=20; mean weight, 16±1 g; ORIENT BIO, Inc.) aged 5-6 weeks, respectively. The mice were housed in a pathogen-free animal facility with a 12 h light/dark cycle at 20-24˚C with 45-55% humidity and allowed free access to food and water. All animals were examined for tumor formation and growth every 3 days. To produce OSCC xenograft models, 100 μl of the tumor resuspended in Dulbecco's Phosphate Buffered Saline (D-PBS) was injected subcutaneously into the flank. After ~3 weeks, when the tumor size approached 10^2 mm^3, and the tumor volume was calculated by $V=(L \times W^2)/2$ where V=volume (mm^3); L=the largest dimension (mm); W=perpendicular diameter (mm), the mice were anesthetized via inhalation of isoflurane (IFRAN LIQ., Hana Pharm Co., Ltd.) with an induction concentration of 4-5% and a maintenance concentration of 2-3%, and the tumors xenografts form each mouse were removed. The humane endpoint of the experiment was reached when any of the following criteria applies: The tumor's largest diameter reaches <20 mm, the tumor weight exceeds 10% of the animals' body weight, the body weight losses >20% of animals' body weight or the animal stops eating and is deemed to be in poor health. After the experiment was completed, all mice were sedated with a CO_2/O_2 mixture (70/30%). Once the mice lost consciousness, they were euthanized with 100% CO_2. Euthanasia was performed in a chamber for 5 min, and death was confirmed by monitoring breathing, heart beating and pupil dilation for an additional 5 min. Nude mouse tumors were explanted for protein and RNA extraction, embedded in paraffin blocks, and frozen. The present study was approved (approval no. GWNUIRB-2020-36-1) by the Committee for Ethical Review of Research of Gangneung-Wonju National University (Gangneung-si, Korea) and conducted from December 2020 to January 2023.

Terminal deoxynucleotidyl-transferase-mediated dUTP nick end labeling (TUNEL) assay. To observe cell death *in vivo*, a TUNEL assay was performed using the *in situ* Cell Death Detection kit (cat. no. 12156792910; Roche Diagnostics) following the manufacturer's protocol. Briefly, frozen tissues were cryo-sectioned at a thickness of 7 μm using a cryostat microtome (Leica Microsystems, Inc.). The sections were fixed on slides with 4% paraformaldehyde for 20 min at RT and then washed thrice with PBS. The slides were then permeabilized with 0.1% sodium citrate for 2 min on ice and washed thrice with PBS. The samples were added to the TUNEL reaction mixture, incubated at 37˚C, without a CO_2 incubator, for 1 h, and washed thrice with PBS. For quantification, at least seven images were obtained, and the samples were analyzed using a fluorescence microscope (BX53; Olympus Corporation) at x40 magnification. The experiments were performed in triplicate.

2,5-diphenyl-2H-tetrazolium bromide (MTT) assay. The MTT assay was performed to analyze the effect of doxorubicin (DOX) on DNA damage mediated by the expression of PTTG1 and p21 in OSCC cell lines. Briefly, OSCC cells were seeded in a 96-well plate and cultured at 37˚C in a 5% CO_2 humidified incubator. After 24 h, the cells were treated with 0.05, 0.5, 5, 50 and 100 μM of DOX (cat. no. D4193; Tokyo Chemical Industry Co., Ltd.) for 24 h and 200 μl DMSO (cat. no. 276855; Sigma-Aldrich; Merck KGaA) for 30 min. Absorbance at 570 nm was then measured using and enzyme-linked immunosorbent assay (ELISA) microplate reader (Molecular Devices, LLC). All experiments were repeated at least three times.

Statistical analyses. All assays were performed in triplicate, and the data are presented as the mean ± standard error (SE) of the mean. Differences in test variables between the control and experimental groups were analyzed using an unpaired Student's t-test or one-way ANOVA, followed by Dunnett's post hoc test. $^*P<0.05$ was considered to indicate a statistically significant difference. Statistical analyses were performed using SPSS (version 20.0; IBM Corp.) and GraphPad Prism 9 (GraphPad Software; Dotmatics).

Results

PTTG1 is overexpressed in OSCC tissues. To investigate the expression and potential role of PTTG1 in OSCC, IHC was performed on 32 pairs of OSCC and adjacent healthy tissue samples. PTTG1 expression was significantly higher in OSCC tissues than in healthy tissues (Fig. 1A). Samples from patients with OSCC were further examined using RT-qPCR and western blot analysis which confirmed that PTTG1 was significantly overexpressed in tumors compared with that in healthy tissues (Fig. 1B and C; protein fold change: 2.10, 2.14, 2.10 and 2.00, respectively, compared with non-tumor tissues). In addition, PTTG1 was expressed in HSC-2 and SCC-9, two OSCC cell lines. Interestingly, the expression

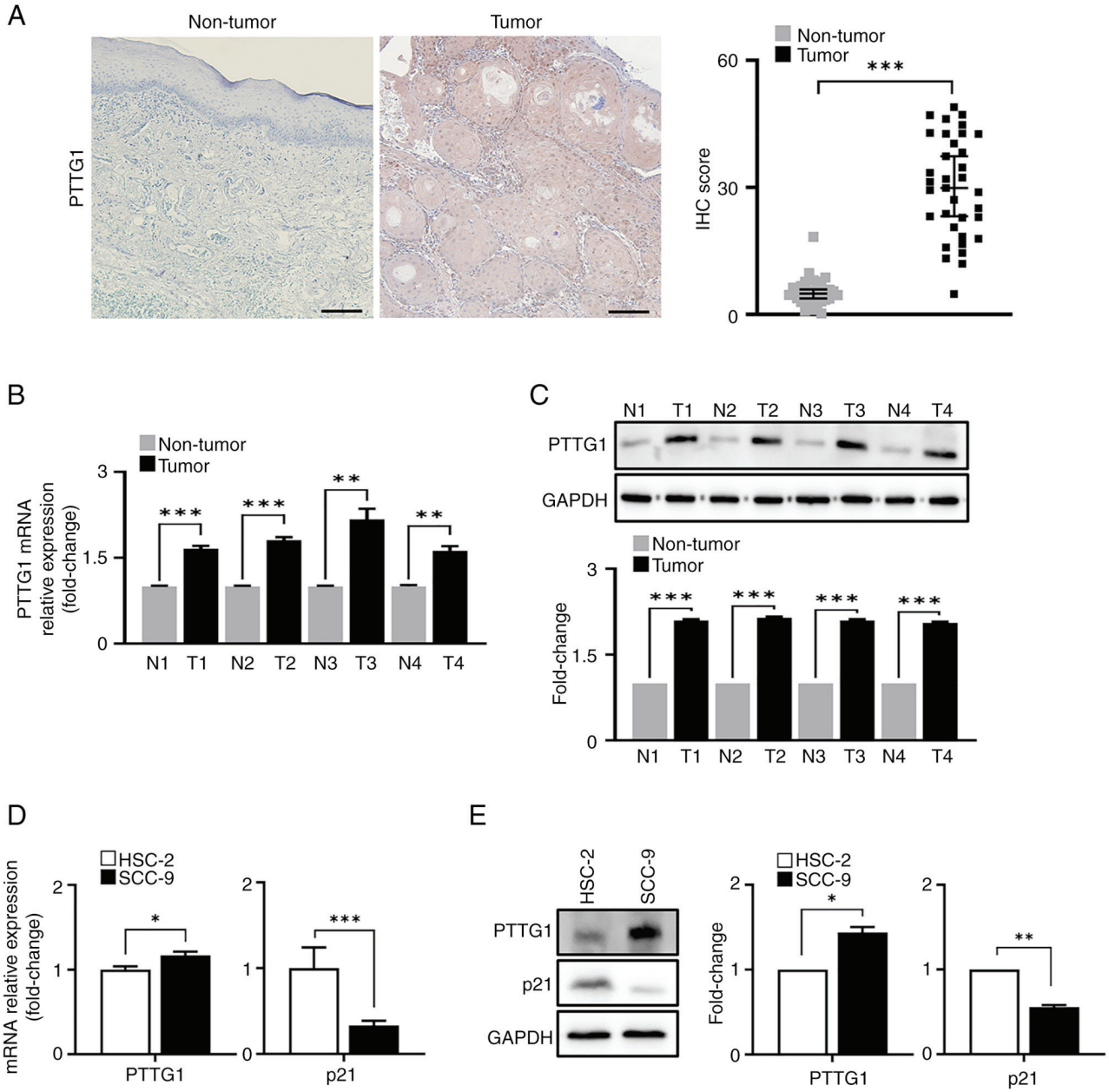

Figure 1. PTTG1 expression in OSCC tissues and cells. (A) Representative images (left) and quantification (right) of PTTG1 immunohistochemistry staining in healthy (n=32) and OSCC tissues (n=32). Scale bar, 100 μm; original magnification, x20. (B) PTTG1 expression was analyzed by RT-qPCR for the pooled OSCC tissue samples. *P<0.05, **P<0.01 and ***P<0.001 vs. non-tumor. (C) Protein expression of PTTG1 in the pooled OSCC samples revealed by western blotting. The upper panel shows the membranes stained with antibodies, with GAPDH as an internal control, and the lower panel shows the relative quantification of protein expression. (D) mRNA and (E) protein expression (left) and fold change (right) of PTTG1 and p21 were analyzed by RT-qPCR and western blotting in OSCC cell lines. *P<0.05, **P<0.01 and ***P<0.001 vs. HSC-2 cell lines using Student's t-test. All experiments were performed in triplicate. PTTG1, pituitary tumor-transforming gene 1; OSCC, oral squamous cell carcinoma; RT-qPCR, reverse transcription quantitative PCR; N, non-tumor; T, tumor.

of the anti-oncogene p21, which is associated with several key characteristics of cellular senescence (i.e., a modified transcriptome, DNA damage, and SASP) (30,31) exhibited an opposite pattern in HSC-2 and SCC-9 cell lines in contrast to that of PTTG1 (Fig. 1D and E; protein fold change: 1.44 and 0.56, respectively, between HSC-2 and SCC-9 cells). The results of the independent analyses indicated that PTTG1 is an oncogene highly expressed in both OSCC tissues and cells.

PTTG1 depletion in OSCC cells suppresses cell proliferation and promotes apoptosis via cell cycle arrest. To evaluate the effect of PTTG1 on OSCC cell proliferation, the expression of PTTG1 was inhibited using siRNA. The mRNA and protein expression of PTTG1 was significantly downregulated in HSC-2, SCC-9 and YD-10B cells transfected with siRNA-PTTG1 compared with levels in those transfected with the vehicle control (Figs. 2A and S1A). Furthermore, the expression of PCNA, a DNA replication marker (32), was significantly reduced in both OSCC cell lines transfected with siRNA-PTTG1 compared with levels in those transfected with the vehicle control (Figs. 2B and S1B). The percentage of DNA synthesis was significantly suppressed in HSC-2 and SCC-9 cells transfected with siRNA-PTTG1, leading to a decrease in cell viability, compared with that in cells transfected

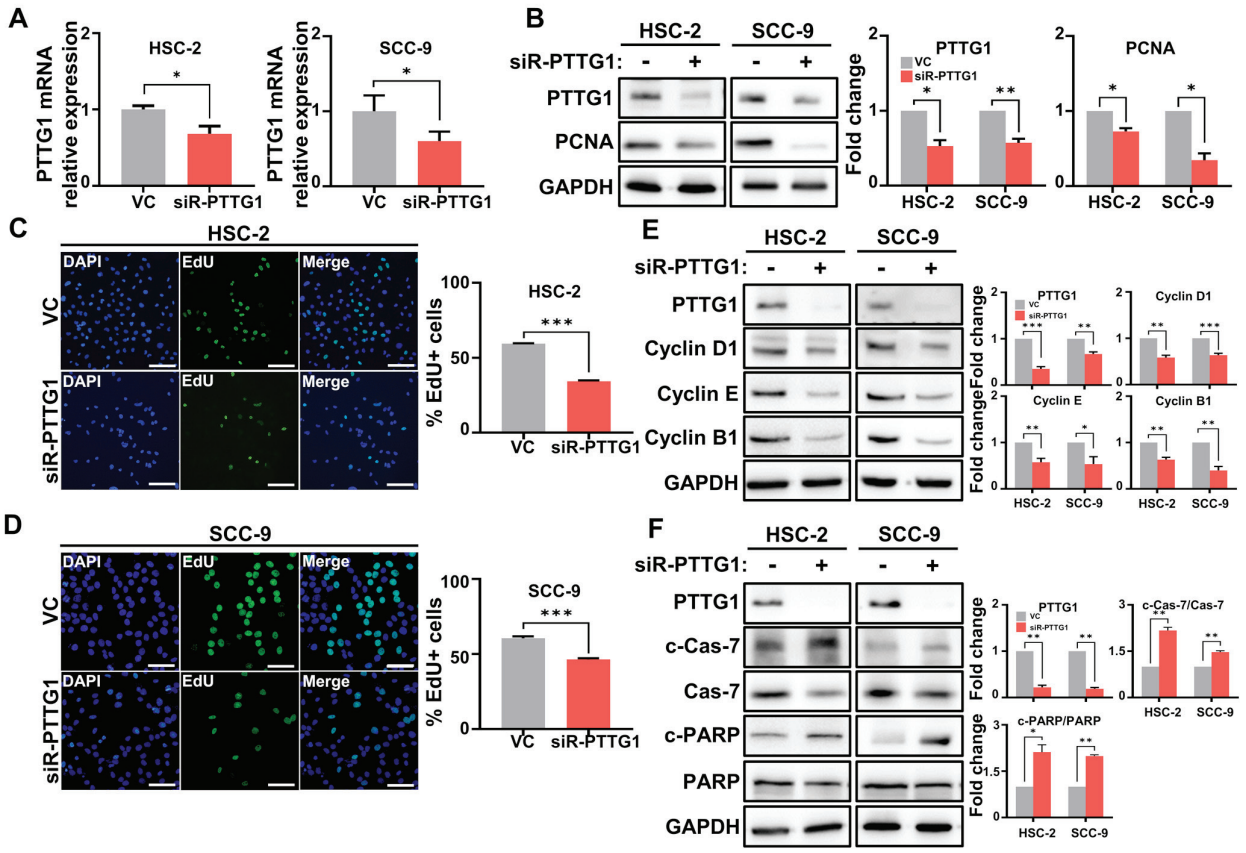

Figure 2. PTTG1 expression in relation to cell proliferation, cell cycle and apoptosis in OSCC cells. (A) PTTG1 expression was analyzed by reverse transcription quantitative PCR in OSCC cells. (B) Protein expression of PTTG1 and PCNA in OSCC cell lines revealed by western blotting. The left panel shows the membranes stained with antibodies, with GAPDH as an internal control, and the right panel shows the relative quantification of protein expression. (C and D) Representative images of cell proliferation ability (left) and quantification (right) of PTTG1 using the EdU assay in the (C) HSC-2 and (D) SCC-9 cell lines (scale bars, 100 μm and 50 μm, respectively; original magnification, x40). The percentages of HSC-2 and SCC-9 cells treated with VC or siR-PTTG1 were determined by EdU incorporation (green) and DAPI (blue). (E) Protein expression (left) and the fold change (right) of cell cycle markers, including cyclins D1, E, and B1 in OSCC cells. (F) Protein expression (left) and fold change (right) related to apoptosis markers, including Cas-7, c-Cas-7, and c-PARP in OSCC cells. *P<0.05, **P<0.01 and ***P<0.001 vs. VC using Student's t-test. All experiments were performed in triplicate. PTTG1, pituitary tumor-transforming gene 1; OSCC, oral squamous cell carcinoma; PCNA, proliferating cell nuclear antigen; VC, vehicle control; siR-PTTG1, small interfering RNA-PTTG1; EdU, 5-ethynyl-2'-deoxyuridine; Cas-7, Caspase-7; c-, cleaved-; PARP, poly (ADP-ribose) polymerase.

with the vehicle control (Fig. 2C and D). Additionally, cyclins D1, B1 and E1, which are responsible for cell proliferation, cell division and DNA replication, respectively, were significantly downregulated in both OSCC cell lines transfected with siRNA-PTTG1 compared with levels in those transfected with the vehicle control (Figs. 2E and S1C). Aberrant changes in the cell cycle in cancer cells lead to an imbalance between cell survival and apoptosis (33). In the present study, the expression ratio of apoptotic markers (including c-Cas-7 and c-PARP) was significantly increased in both OSCC cell lines transfected with siRNA-PTTG1 compared with levels in those transfected with the vehicle control (Figs. 2F and S1D). These findings suggested that PTTG1 depletion in OSCC cells restricts cell proliferation and promotes cell death through cell cycle arrest.

PTTG1 depletion in OSCC cells promotes cellular senescence via p21. p21 is a cyclin-dependent kinase inhibitor and a senescence regulator in senescent cells, where its activation maintains stable cell cycle arrest (25). To determine whether cell cycle arrest caused by PTTG1 results in cellular senescence, alterations in senescent phenotypes were evaluated following PTTG1 knockdown. The mRNA and protein expression of p21 was significantly increased in both cell lines transfected with siRNA-PTTG1 compared with levels in those transfected with the vehicle control (Fig. 3A and B). Moreover, intracellular SA-β-gal significantly accumulated in both OSCC cell lines transfected with siRNA-PTTG1 compared with that in those transfected with vehicle control (Fig. 3C). To understand the mechanism underlying apoptosis induction in senescent cells following PTTG1 knockdown and to test whether an increased DNA damage response (DDR) causes this effect after knockdown, the phosphorylation levels of ATM and ATR, which are involved in the DDR, were evaluated. It was found that PTTG1 knockdown in the two OSCC cell lines led to a substantial increase in the phosphorylation of these proteins (Fig. 3D). Furthermore, there was a significant increase in the number of γH2AX foci in the nucleus of PTTG1 knockdown cells compared with that in those transfected with the vehicle control, where only a few γH2AX foci were observed (Fig. 3E and F). In the YD-10B cell line, it was observed that γH2AX expression and SA-β-gal accumulation increased compared with the vehicle control after PTTG1 knockdown (Fig. S2). Furthermore, in the HSC-2 and SCC-9 cell lines, PTTG1 knockdown resulted in decreased

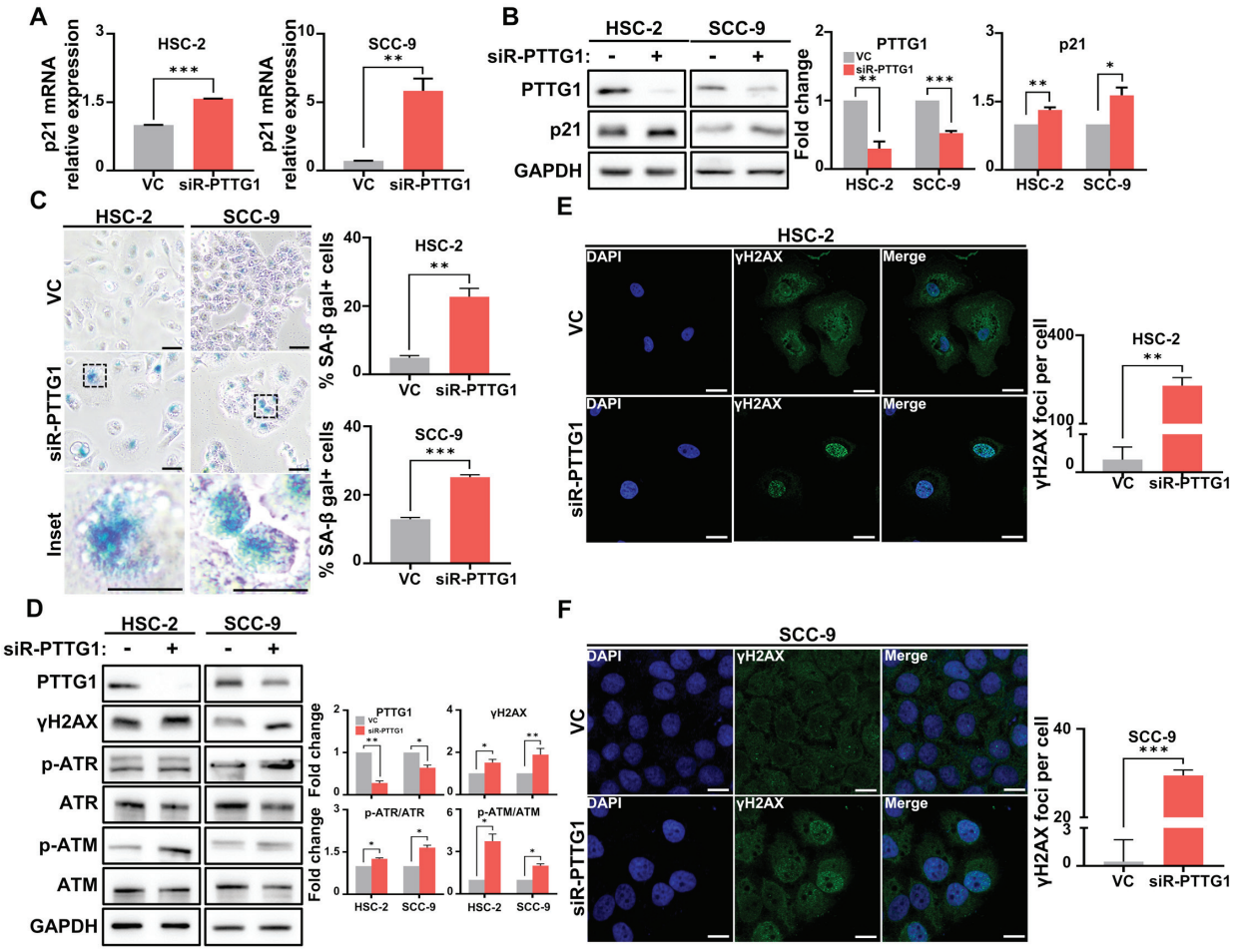

Figure 3. The effect of PTTG1 on cellular senescence and DNA damage in OSCC. (A) mRNA expression of p21 was analyzed by reverse transcription quantitative PCR in OSCC cells. (B) Protein expression (left) and quantification (right) of PTTG1 and p21 were analyzed by western blotting in OSCC cells. (C) Representative images (left) and numbers (right) of cellular senescence in OSCC cells detected by senescence-associated β-galactosidase staining (blue). The percentages of HSC-2 and SCC-9 were determined by β-galactosidase incorporation (scale bars, 50 μm and 200 μm, respectively; original magnification, x40). (D) Protein expression (left) and fold change (right) related to DNA damage, including γH2AX, p-ATR and p-ATM in OSCC cells. GAPDH was used as an internal control. (E) Representative images (left) and numbers (right) of chromosomal damage detected by γH2AX staining in HSC-2 cells (scale bar, 50 μm; original magnification, x63). (F) Representative images (left) and numbers (right) of chromosomal damage detected by γH2AX staining in SCC-9 cells (scale bar, 250 μm; original magnification, x63). *P<0.05, **P<0.01 and ***P<0.001 vs. VC using Student's t-test. All experiments were performed in triplicate. PTTG1, pituitary tumor-transforming gene 1; OSCC, oral squamous cell carcinoma; γH2AX, phosphorylated histone H2AX; ATR, ataxia telangiectasia and Rad3-related protein; p-, phosphorylated; ATM, ataxia telangiectasia mutant; siR-PTTG1, small interfering RNA-PTTG1; SA-β gal, senescence-associated beta-galactosidase; VC, vehicle control.

p53 expression and increased p-Rb expression compared to the vehicle control (Fig. S3). These findings suggested that loss of PTTG1 promotes DNA damage in a p21-dependent manner, followed by cellular senescence regardless of cell types.

PTTG1 depletion in OSCC cells promotes apoptosis via DNA damage in vivo. To verify the effect of PTTG1 on tumor progression, 6-week-old nude mice were subcutaneously injected with 2x10^{6} vehicle control-treated or PTTG1-knockdown HSC-2 or SCC-9 cells. Tumor growth, weight, DNA damage and apoptosis were analyzed to determine the effect of PTTG1 on tumor progression (Fig. 4A). Compared with that in the vehicle control-treated group, a steady reduction in tumor size was observed in the groups injected with PTTG1-knockdown HSC-2 and SCC-9 cell lines starting from 15 days after injection (Fig. 4B). The largest tumor observed in the SCC-9 VC group had a maximum diameter of 14.06 mm and a volume of 12.6 mm (V=1116 mm^{3}). Moreover, the groups injected with the PTTG1-knockdown cell lines showed a statistically significant decrease in tumor weight 3 weeks after cell injection compared with that in the vehicle control group (Fig. 4C). Immunoblotting results revealed that PTTG1 knockdown significantly reduced the expression of PCNA, a cell proliferation marker, and elevated the expression of p21 (senescence), c-Cas-7 (apoptosis), markers of γH2AX p-ATR and p-ATM (DNA damage), compared with that in the vehicle control-treated group (Fig. 4D). To examine whether the reduction in tumor growth by PTTG1 knockdown was associated with DNA damage-dependent cancer cell apoptosis, a TUNEL assay was performed to measure DNA breaks in cells undergoing apoptosis (34). In the vehicle control group, the nuclei of cells present in the tumor tissues exhibited a negligible number of DNA breaks. Conversely, tumor tissues injected with PTTG1-knockdown HSC-2 and SCC-9 cells displayed a significant increase in DNA breaks, similar to the effects observed with DNA-damaging chemicals *in vitro* (Figs. 4E, F

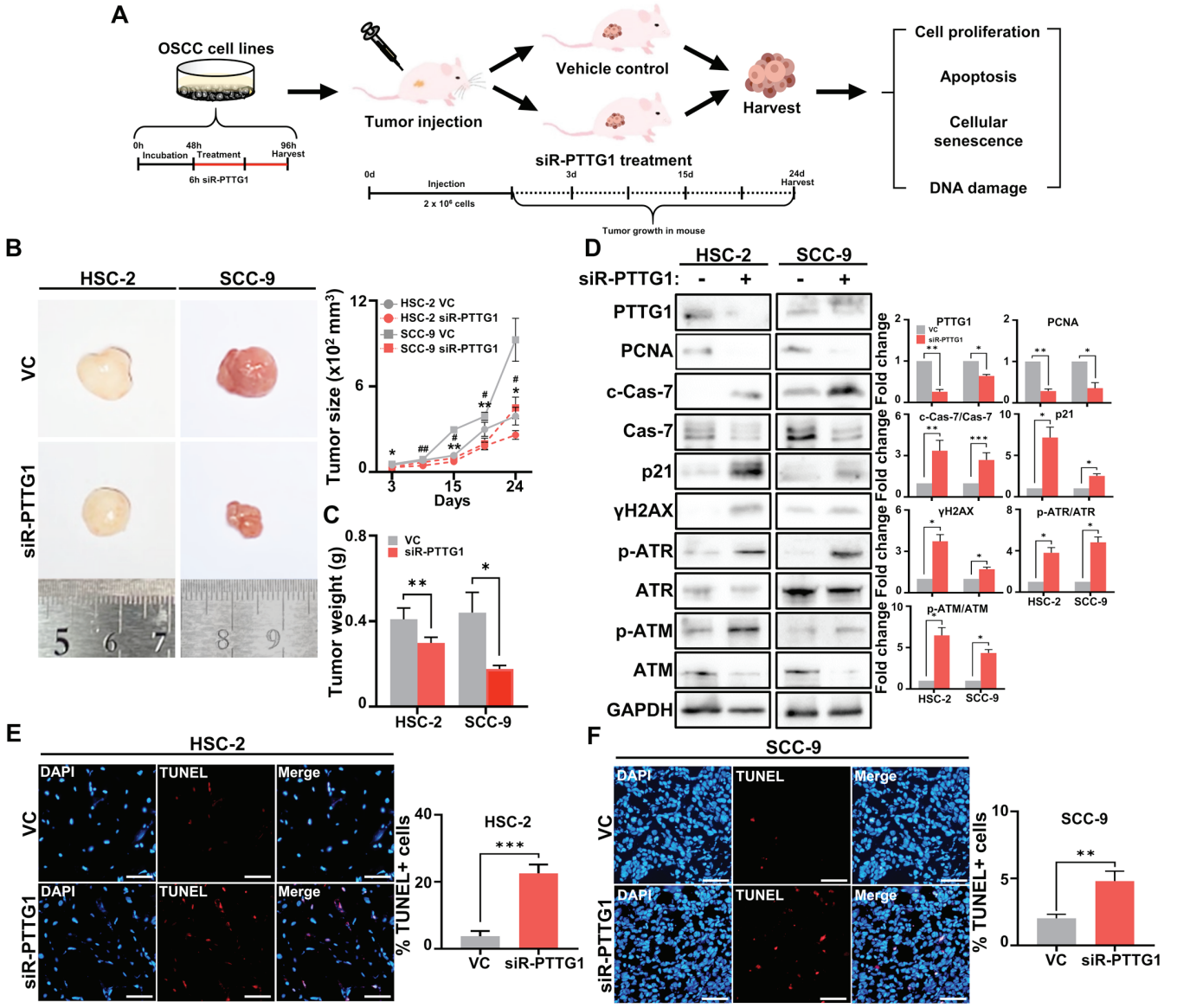

Figure 4. The effect of PTTG1 downregulation on tumor growth *in vivo*. (A) A schematic diagram of transfection *in vivo*. (B) Representative images of tumor sizes *in vivo*. The tumor size of each group was depicted graphically *in vivo*. (scale bar, 500 mm). (C) Tumor weights of each group *in vivo*. (D) Protein expression (left) and fold change (right) related to cell proliferation, apoptosis, cellular senescence and DNA damage, including PCNA, c-Cas-7, p21, γH2AX and p-ATM in OSCC cell lines. GAPDH was used as an internal control. (E and F) Representative images (left) and numbers (right) of apoptotic DNA damage analyzed by TUNEL assay (red) and DAPI (blue) in (E) HSC-2 and (F) SCC-9 cells (scale bar, 50 μm; original magnification, x20). *P<0.05, **P<0.01, ***P<0.001, $^{\#}$P<0.05 and $^{\#\#}$P<0.01 vs. VC using Student's t-test. All experiments were performed in triplicate. PTTG1, pituitary tumor-transforming gene 1; PCNA, proliferating cell nuclear antigen; c-Cas-7, cleaved Caspase-7; γH2AX, phosphorylated histone H2AX; ATM, ataxia telangiectasia mutant; p-, phosphorylated; Cas-7, Caspase-7; ATR, ataxia telangiectasia and Rad3-related protein; ATM, ataxia telangiectasia mutant; OSCC, oral squamous cell carcinoma; TUNEL, terminal deoxynucleotidyl transferase-mediated dUTP nick end labeling; VC, vehicle control.

and S4). Thus, these findings suggested that PTTG1 expression plays a crucial role in regulating tumor growth and apoptosis and that these effects are mediated by DNA damage.

Discussion

Numerous studies have investigated the role of PTTG1 in promoting the malignant progression of cancer through various mechanisms (35-37). These studies emphasize the crucial significance of PTTG1 in tumor progression and further support the present and related previous studies, which identified a role for PTTG1 in OSCC growth and metastasis. It was previously demonstrated by the authors that suppressing the expression of PTTG1 led to a significant reduction in the migration and invasion abilities of the OSCC cell lines YD-10B and YD-15. However, the differential effects of PTTG1 on the growth of YD-10B and YD-15 cells are attributed to the expression of p53 (38), which was not expressed in YD-10B cells but was strongly expressed in YD-15 cells. p53 is a potent tumor suppressor gene, and mutations in this gene have been observed in most cancers. These mutations disrupt the function of antitumor genes and contribute to cancer progression facilitated by oncogenes (39). In the YD-10B cell line, independent of p53 expression, PTTG1 knockdown significantly inhibited PCNA expression compared with that in the vehicle control (Fig. S1A and B, P<0.05). Furthermore, PTTG1 knockdown

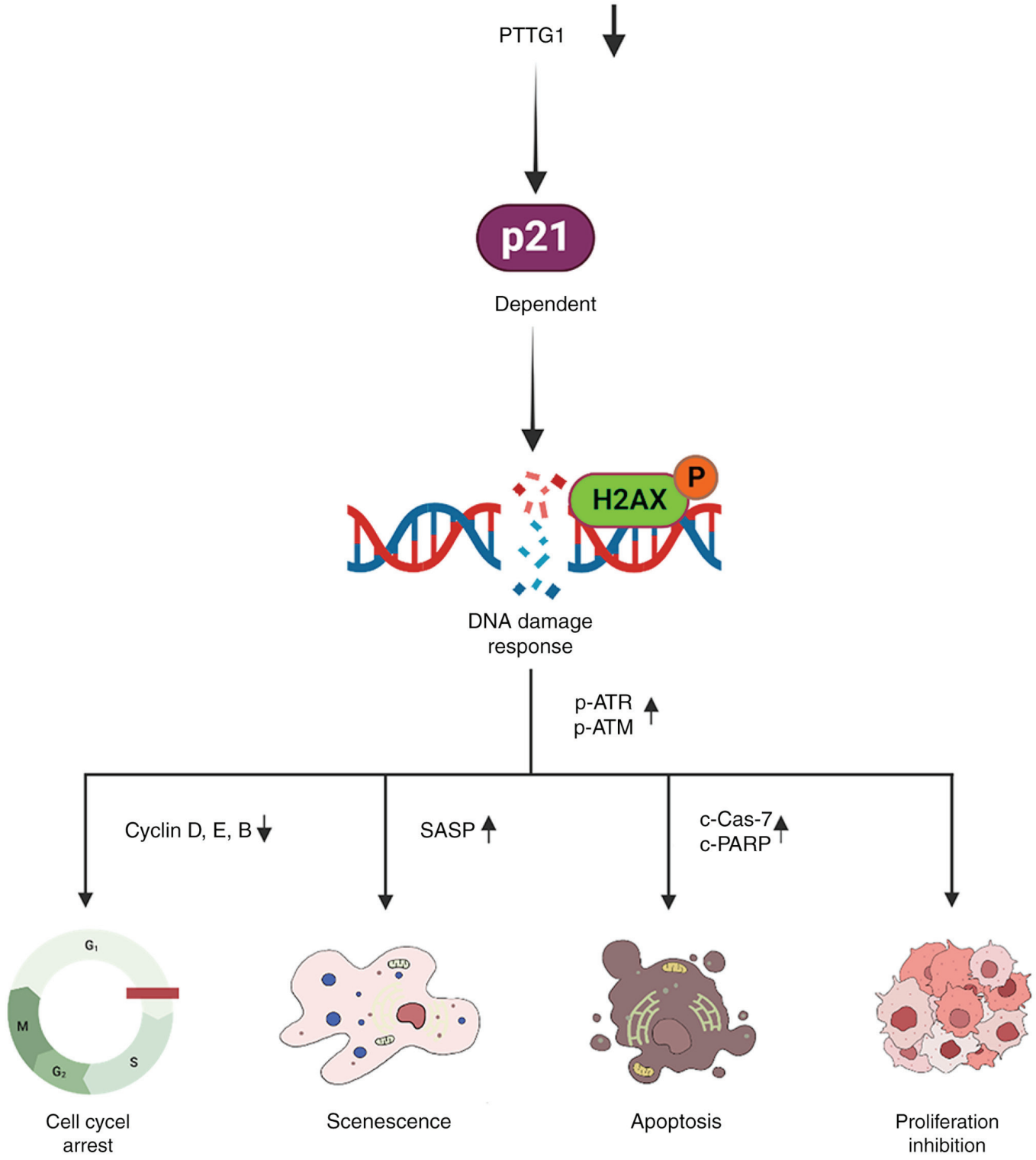

Figure 5. A schematic model of DNA damage induced by the downregulation of PTTG1 in oral squamous cell carcinoma. PTTG1, pituitary tumor-transforming gene 1; phosphorylated histone H2AX; p-ATR, Phosphorylated ataxia telangiectasia and Rad3-related protein; p-ATM, phosphorylated ataxia telangiectasia mutant; SASP, senescence-associated secretory phenotype; c-Cas-7, cleaved Caspase-7; c-PARP, cleaved poly (ADP-ribose) polymerase.

resulted in inhibition of proteins involved in the cell cycle or induction of apoptotic markers (Fig. S1C and D). Interestingly, consistent with the findings observed in YD-10B, PTTG1 knockdown induced DNA damage (Fig. S2A) and cellular senescence (Fig. S2B), which is in contrast with observations in the corresponding vehicle control. Therefore, in the present study, the HSC-2 and SCC-9 cell lines were utilized, both of which harbor p53 mutations, to comprehensively investigate the role of PTTG1 in OSCC progression (40,41).

In the present study, PTTG1 was observed overexpression in patients with OSCC and it was revealed that PTTG1 negatively regulates the expression of p21, leading to stable cell cycle arrest. The suppression of PTTG1 expression in OSCC cells resulted in irreversible DNA damage and sustained

senescence. However, the molecular mechanisms underlying the regulation of the p21-dependent pathway by PTTG1 require further investigation. Moreover, whether the DDR pathway is activated in OSCC following DNA damage induced by PTTG1 inhibition requires further investigation to provide a comprehensive understanding of the molecular mechanisms involved. Finally, the present *in vivo* results demonstrated that inhibiting PTTG1 expression induces apoptosis in OSCC cells. Therefore, the current study provided novel evidence supporting the significant role of PTTG1 in OSCC proliferation and metastasis through cell cycle arrest, DNA damage and cell death mediated by p21 (Fig. 5).

DNA damage refers to the disruption or breakage of DNA strands due to the generation of abnormal nucleotides or nucleotide fragments. This can be induced by various intrinsic or extrinsic factors, including ionizing radiation, reactive oxygen species and drugs, in normal cells (42). Persistent DNA damage triggers the activation of cellular processes, such as apoptosis or senescence, which prevent the replication of a damaged genome (43). In contrast to normal cells, cancer cells frequently arise because of replication stress induced by oncogenes. Additionally, DDR mechanisms, which continuously repair DNA damage to prevent senescence and apoptosis, prolong the survival of cancer cells (44). Therefore, most antitumor therapeutic strategies aim to inhibit the growth of cancer cells, induce apoptosis, and impose continuous and significant DNA damage to fundamentally block the DDR mechanism (45). Following DNA damage stress and DNA double-strand breaks, ATM and ATR undergo excessive phosphorylation, which leads to phosphorylation of the histone variant H2AX at the Ser^{139} residue, resulting in the formation of p-H2AX (γH2AX) (46). γH2AX plays a crucial role in inducing cell apoptosis in cancer cells (47). Therefore, p53 may play a central role in determining the spontaneous fate of cells following DNA damage. Recently, Engeland et al (48) demonstrated that p53, during activation by DNA damage, upregulates p21 expression and induces cell cycle arrest via Rb-E2F complex formation. However, in the present study, it was found that PTTG1 downregulation led to the activation of p21 expression and the downregulation of p53 expression. PTTG1-induced senescence and apoptosis in OSCC cells were regulated independently of p53 and Rb (Figs. 3B and S3). Similar results regarding cancer apoptosis through p53-independent induction of p21 have been reported by other research groups in studies on prostate and liver cancers (49,50). These findings further support the observation of p53-independent senescence and apoptosis in OSCC cells. In addition, DOX was used to investigate changes in the expression of PTTG1 and p21 following anticancer drug treatment. DOX is known to cause DNA double-strand breaks and is currently used as a clinical anticancer treatment (51,52). Therefore, to investigate the appropriate concentration of DOX, IC_{50} values in HSC-2 (2.7 μM) and SCC-9 cells (27 μM) were analyzed MTT assays (Fig. S4A and B). The present results identified that mRNA expression of PTTG1 was significantly decreased after DOX treatment in both cell lines (Fig. S4C). Conversely, the mRNA expression of p21 was significantly increased in both cell lines (Fig. S4D). In addition, it was found that DOX treatment in the two OSCC cell lines led to a substantial increase in the number of γH2AX foci in the nucleus compared with that in control (Fig. S4E and F). These results suggested that the p21-dependent expression of PTTG1 may elucidate the mechanism of anticancer treatment. However, the current results also have certain limitations. First, it is needed to analyze the expression of PTTG1 in OSCC patients who underwent chemotherapy and radiation therapy. Second, it is needed to identify the mechanisms that induce senescence and apoptosis in OSCC though p21-only silencing in both *in vitro* and *in vivo* experiments. Lastly, the role of p21-dependent PTTG1 after chemotherapy in *in vitro* experiments needs to be investigated in future studies.

Taken together, the findings of the present study support the proposed role of PTTG1 as an oncogene and demonstrated that inducing DNA damage through PTTG1 downregulation suppresses OSCC growth and metastasis by promoting senescence and apoptosis in a p53-independent and p21-dependent manner. These novel insights contribute to understanding of the mechanisms underlying OSCC development and metastasis and may open avenues for the development of diagnostic and therapeutic strategies for OSCC.

Acknowledgements

Not applicable.

Funding

The present study was supported by the Basic Science Research Program through a National Research Foundation of Korea grant funded by the Korean Government (MSIT) (grant no. 2020R1C1C1004007) and the Ministry of Education, Science, and Technology (grant no. 2019R1I1A33A01057886).

Availability of data and materials

The data generated in the present study may be requested from the corresponding author.

Authors' contributions

SP and JC designed the study and wrote the manuscript. SP and SK performed the experiments. MYK and SSL collected clinical specimens and wrote the manuscript. SP and SK revised the paper. SP, SK and JC confirm the authenticity of all the raw data. All authors read and approved the final manuscript.

Ethics approval and consent to participate

The present study was approved by the Committee for Ethical Review of Research of Gangneung-Wonju National University (approval no. GWNUIRB-2020-26-1; Gangneung-si, Korea). Written informed consent was provided by all patients before surgery. Animal studies were approved by the Gangneung-Wonju National University Ethics Committee on Animal Experiments (approval no. GWNUIRB-2020-36-1; Gangneung-si, Korea).

Patient consent for publication

Not applicable.

Competing interests

The authors declare that they have no competing interests.

References

1. No authors listed: Oral cancer-the fight must go on against all odds…. Evid Based Dent 23: 4-5, 2022.
2. Sung H, Ferlay J, Siegel RL, Laversanne M, Soerjomataram I, Jemal A and Bray F: Global cancer statistics 2020: GLOBOCAN estimates of incidence and mortality worldwide for 36 cancers in 185 countries. CA Cancer J Clin 71: 209-249, 2021.
3. Johnson DE, Burtness B, Leemans CR, Lui VWY, Bauman JE and Grandis JR: Head and neck squamous cell carcinoma. Nat Rev Dis Primers 6: 92, 2020.
4. Kuo TJ, Jean YH, Shih PC, Cheng SY, Kuo HM, Lee YT, Lai YC, Tseng CC, Chen WF and Wen ZH: Stellettin B-induced oral cancer cell death via endoplasmic reticulum stress-mitochondrial apoptotic and autophagic signaling pathway. Int J Mol Sci 23: 8813, 2022.
5. Kruijtzer CM, Beijnen JH and Schellens JH: Improvement of oral drug treatment by temporary inhibition of drug transporters and/or cytochrome P450 in the gastrointestinal tract and liver: An overview. Oncologist 7: 516-530, 2002.
6. Dobler C, Jost T, Hecht M, Fietkau R and Distel L: Senescence induction by combined ionizing radiation and DNA damage response inhibitors in head and neck squamous cell carcinoma cells. Cells 9: 2012, 2020.
7. Pei L and Melmed S: Isolation and characterization of a pituitary tumor-transforming gene (PTTG). Mol Endocrinol 11: 433-441, 1997.
8. Jallepalli PV, Waizenegger IC, Bunz F, Langer S, Speicher MR, Peters JM, Kinzler KW, Vogelstein B and Lengauer C: Securin is required for chromosomal stability in human cells. Cell 105: 445-457, 2001.
9. Vlotides G, Eigler T and Melmed S: Pituitary tumor-transforming gene: Physiology and implications for tumorigenesis. Endocr Rev 28: 165-186, 2007.
10. Teveroni E, Di Nicuolo F, Bianchetti G, Epstein AL, Grande G, Maulucci G, De Spirito M, Pontecorvi A, Milardi D and Mancini F: Nuclear localization of PTTG1 promotes migration and invasion of seminoma tumor through activation of MMP-2. Cancers (Basel) 13: 212, 2021.
11. Wang Z, Yu R and Melmed S: Mice lacking pituitary tumor transforming gene show testicular and splenic hypoplasia, thymic hyperplasia, thrombocytopenia, aberrant cell cycle progression, and premature centromere division. Mol Endocrinol 15: 1870-1879, 2001.
12. Lai Y, Xin D, Bai J, Mao Z and Na Y: The important anti-apoptotic role and its regulation mechanism of PTTG1 in UV-induced apoptosis. J Biochem Mol Biol 40: 966-972, 2007.
13. Kim DS, Franklyn JA, Smith VE, Stratford AL, Pemberton HN, Warfield A, Watkinson JC, Ishmail T, Wakelam MJ and McCabe CJ: Securin induces genetic instability in colorectal cancer by inhibiting double-stranded DNA repair activity. Carcinogenesis 28: 749-759, 2007.
14. Read ML, Fong JC, Modasia B, Fletcher A, Imruetaicharoenchoke W, Thompson RJ, Nieto H, Reynolds JJ, Bacon A, Mallick U, *et al*: Elevated PTTG and PBF predicts poor patient outcome and modulates DNA damage response genes in thyroid cancer. Oncogene 36: 5296-5308, 2017.
15. Pei L: Identification of c-myc as a down-stream target for pituitary tumor-transforming gene. J Biol Chem 276: 8484-8491, 2001.
16. Bernal JA, Luna R, Espina A, Lázaro I, Ramos-Morales F, Romero F, Arias C, Silva A, Tortolero M and Pintor-Toro JA: Human securin interacts with p53 and modulates p53-mediated transcriptional activity and apoptosis. Nat Genet 32: 306-311, 2002.
17. Liao LJ, Hsu YH, Yu CH, Chiang CP, Jhan JR, Chang LC, Lin JJ and Lou PJ: Association of pituitary tumor transforming gene expression with early oral tumorigenesis and malignant progression of precancerous lesions. Head Neck 33: 719-726, 2011.
18. Zhang E, Liu S, Xu Z, Huang S, Tan X, Sun C and Lu L: Pituitary tumor-transforming gene 1 (PTTG1) is overexpressed in oral squamous cell carcinoma (OSCC) and promotes migration, invasion and epithelial-mesenchymal transition (EMT) in SCC15 cells. Tumour Biol 35: 8801-8811, 2014.
19. Piskorz WM and Cechowska-Pasko M: Senescence of tumor cells in anticancer therapy-beneficial and detrimental effects. Int J Mol Sci 23: 11082, 2022.
20. Kuilman T, Michaloglou C, Mooi WJ and Peeper DS: The essence of senescence. Genes Dev 24: 2463-2479, 2010.
21. Campisi J and d'Adda di Fagagna F: Cellular senescence: When bad things happen to good cells. Nat Rev Mol Cell Biol 8: 729-740, 2007.
22. Childs BG, Baker DJ, Kirkland JL, Campisi J and van Deursen JM: Senescence and apoptosis: Dueling or complementary cell fates? EMBO Rep 15: 1139-1153, 2014.
23. Gorgoulis V, Adams PD, Alimonti A, Bennett DC, Bischof O, Bishop C, Campisi J, Collado M, Evangelou K, Ferbeyre G, *et al*: Cellular senescence: Defining a path forward. Cell 179: 813-827, 2019.
24. Hernandez-Segura A, Nehme J and Demaria M: Hallmarks of cellular senescence. Trends Cell Biol 28: 436-453, 2018.
25. Herranz N and Gil J: Mechanisms and functions of cellular senescence. J Clin Invest 128: 1238-1246, 2018.
26. HAYFLICK L: THE LIMITED IN VITRO LIFETIME OF HUMAN DIPLOID CELL STRAINS. Exp Cell Res 37: 614-636, 1965.
27. Chen YC, Hsieh HH, Chang HC, Wang HC, Lin WJ and Lin JJ: CDC25B induces cellular senescence and correlates with tumor suppression in a p53-dependent manner. J Biol Chem 296: 100564, 2021.
28. Jung SH, Hwang HJ, Kang D, Park HA, Lee HC, Jeong D, Lee K, Park HJ, Ko YG and Lee JS: mTOR kinase leads to PTEN-loss-induced cellular senescence by phosphorylating p53. Oncogene 38: 1639-1650, 2019.
29. Livak KJ and Schmittgen TD: Analysis of relative gene expression data using real-time quantitative PCR and the 2(-Delta Delta C(T)) Method. Methods 25: 402-408, 2001.
30. Jeoung DI, Tang B and Sonenberg M: Induction of tumor suppressor p21 protein by kinase inhibitors in MCF-7 cells. Biochem Biophys Res Commun 214: 361-366, 1995.
31. Englund DA, Jolliffe A, Aversa Z, Zhang X, Sturmlechner I, Sakamoto AE, Zeidler JD, Warner GM, McNinch C, White TA, *et al*: p21 induces a senescence program and skeletal muscle dysfunction. Mol Metab 67: 101652, 2023.
32. Bologna-Molina R, Mosqueda-Taylor A, Molina-Frechero N, Mori-Estevez AD and Sánchez-Acuña G: Comparison of the value of PCNA and Ki-67 as markers of cell proliferation in ameloblastic tumors. Med Oral Patol Oral Cir Bucal 18: e174-e179, 2013.
33. Loftus LV, Amend SR and Pienta KJ: Interplay between cell death and cell proliferation reveals new strategies for cancer therapy. Int J Mol Sci 23: 4723, 2022.
34. Mirzayans R and Murray D: Do TUNEL and other apoptosis assays detect cell death in preclinical studies? Int J Mol Sci 21: 9090, 2020.
35. Meng C, Zou Y, Hong W, Bao C and Jia X: Estrogen-regulated PTTG1 promotes breast cancer progression by regulating cyclin kinase expression. Mol Med 26: 33, 2020.
36. Yang G, Xiog Y, Wang G, Li W, Tang T, Sun J and Li J: miR-374c-5p regulates PTTG1 and inhibits cell growth and metastasis in hepatocellular carcinoma by regulating epithelial-mesenchymal transition. Mol Med Rep 25: 148, 2022.
37. Zhang H, He Z, Qiu L, Wei J, Gong X, Xian M, Chen Z, Cui Y, Fu S, Zhang Z, *et al*: PRR11 promotes cell proliferation by regulating PTTG1 through interacting with E2F1 transcription factor in pan-cancer. Front Mol Biosci 9: 877320, 2022.
38. Lee SS, Choi JH, Lim SM, Kim GJ, Lee SK and Jeon YK: Alteration of pituitary tumor transforming gene 1 by microRNA-186 and 655 regulates invasion ability of human oral squamous cell carcinoma. Int J Mol Sci 22: 1021, 2021.
39. Hu J, Cao J, Topatana W, Juengpanich S, Li S, Zhang B, Shen J, Cai L, Cai X and Chen M: Targeting mutant p53 for cancer therapy: Direct and indirect strategies. J Hematol Oncol 14: 157, 2021.
40. Nakagaki T, Tamura M, Kobashi K, Koyama R, Fukushima H, Ohashi T, Idogawa M, Ogi K, Hiratsuka H, Tokino T and Sasaki Y: Profiling cancer-related gene mutations in oral squamous cell carcinoma from Japanese patients by targeted amplicon sequencing. Oncotarget 8: 59113-59122, 2017.
41. Hauser U, Balz V, Carey TE, Grénman R, Van Lierop A, Scheckenbach K and Bier H: Reliable detection of p53 aberrations in squamous cell carcinomas of the head and neck requires transcript analysis of the entire coding region. Head Neck 24: 868-873, 2002.
42. Alhmoud JF, Woolley JF, Al Moustafa AE and Malki MI: DNA damage/repair management in cancers. Cancers (Basel) 12: 1050, 2020.
43. Yousefzadeh M, Henpita C, Vyas R, Soto-Palma C, Robbins P and Niedernhofer L: DNA damage-how and why we age? Elife 10: e62852, 2021.

44. Trenner A and Sartori AA: Harnessing DNA double-strand break repair for cancer treatment. Front Oncol 9: 1388, 2019.
45. Abuetabh Y, Wu HH, Chai C, Al Yousef H, Persad S, Sergi CM and Leng R: DNA damage response revisited: The p53 family and its regulators provide endless cancer therapy opportunities. Exp Mol Med 54: 1658-1669, 2022.
46. Cimprich KA and Cortez D: ATR: An essential regulator of genome integrity. Nat Rev Mol Cell Biol 9: 616-627, 2008.
47. Bonner WM, Redon CE, Dickey JS, Nakamura AJ, Sedelnikova OA, Solier S and Pommier Y: GammaH2AX and cancer. Nat Rev Cancer 8: 957-967, 2008.
48. Engeland K: Cell cycle regulation: p53-p21-RB signaling. Cell Death Differ 29: 946-960, 2022.
49. Ho CJ, Lin RW, Zhu WH, Wen TK, Hu CJ, Lee YL, Hung TI and Wang C: Transcription-independent and -dependent p53-mediated apoptosis in response to genotoxic and non-genotoxic stress. Cell Death Discov 5: 131, 2019.
50. Lee TK, Lau TC and Ng IO: Doxorubicin-induced apoptosis and chemosensitivity in hepatoma cell lines. Cancer Chemother Pharmacol 49: 78-86, 2002.
51. Kciuk M, Gielecińska A, Mujwar S, Kołat D, Kałuzińska-Kołat Ż, Celik I and Kontek R: Doxorubicin-an agent with multiple mechanisms of anticancer activity. Cells 12: 659, 2023.
52. Yun UJ, Lee JH, Shim J, Yoon K, Goh SH, Yi EH, Ye SK, Lee JS, Lee H, Park J, *et al*: Anti-cancer effect of doxorubicin is mediated by downregulation of HMG-Co A reductase via inhibition of EGFR/Src pathway. Lab Invest 99: 1157-1172, 2019.